Designer ligands. Part 14. Novel Mn(II), Ni(II) and Zn(II) complexes of benzamide- and biphenyl-derived ligands

Kevin W. Wellington,[b] Perry T. Kaye,[a]* and Gareth M. Watkins[a]

[a]*Department of Chemistry, Rhodes University, Grahamstown, 6140, South Africa*
[b]*CSIR Biosciences, Pinelands, Ardeer Road, Modderfontein, 1645, South Africa*
E-mail: P.Kaye@ru.ac.za

Abstract
Manganese(II), nickel(II) and zinc(II) complexes have been prepared using various benzamide- and biphenyl-derived ligands; their structures have been investigated using infrared spectroscopy and it is apparent that, depending on the ligand, the metal centres adopt octahedral, tetrahedral and distorted tetrahedral coordination geometries. The catecholase activity of the manganese(II) complexes has also been evaluated.

Keywords: Manganese(II), nickel(II) and zinc(II) complexes, biomimetic ligands, catalysis

Introduction

Metals play important roles in biological systems and, in earlier papers, we have described the development of biomimetic complexes designed to mimic the active site of tyrosinase,[1] an enzyme capable of *ortho*-hydroxylating phenols (phenolase activity) and oxidising catechols to *ortho*-quinones (catecholase activity).[2,3] Copper[4] and cobalt[5] complexes of novel ligands, prepared in our laboratory, have also been shown to exhibit catecholase activity, and our interests broadened to include other transition metal systems, *viz*., manganese(II), nickel(II) and zinc(II) complexes. Manganese metalloenzymes containing dinuclear active sites[6] have been found to exhibit catalytic activity, while zinc(II) is often present in the active site of hydrolytic metalloenzymes.[7-10] Nickel also plays important roles in biological systems. The first such system to be discovered, the enzyme urease, was isolated from jack beans[11-12] and shown by UV-visible spectroscopy and EXAFS studies to contain two octahedral nickel(II) ions in a nitrogen- and oxygen-donor environment. Nickel has subsequently been found in other enzymes, *viz.,* hydrogenases, CO dehydrogenases and coenzyme F_{430}.[12] It has been found that the hydrogenases and CO dehydrogenases have nickel(III) (low spin d^7) and Fe-S clusters present in their structures,[12] while nickel(II) in coenzyme F_{430}, a cofactor of methyl coenzyme M reductase, exhibits square planar geometry.

We have previously reported the preparation of ligands, which are capable of chelating two metal ions and, in which, the coordinating moieties are separated by biphenyl,[13] 1,10-phenanthroline[14] or acyclic spacers.[15] In this paper, we now discuss: - the synthesis of the selected benzamide derivatives **1a-c**; the capacity of such compounds and of various biphenyl derivatives to serve as multidentate ligands for the preparation of novel Mn(II), Ni(II) and Zn(II) complexes; and the biomimetic catecholase activity of the Mn(II) complexes.

Results and Discussion

The ligands **1a-c** (Scheme 1) were prepared by treating benzoic acid with carbonyl diimidazole (CDI)[13] in dimethylformamide (DMF), followed by the respective primary amines, histamine, 2-(2-aminoethyl)benzimidazole and 2-(2-aminoethyl)pyridine. [Histamine had to be released from its dihydrochloride salt by treatment with sodium methoxide, while 2-(2-aminoethyl)benzimidazole was prepared from 1,2-diaminobenzene and *β*-alanine.[16]] The synthesis of the biphenyl-derived ligand **2**, which also contains imidazolyl groups, has been reported previously.[13] Schemes 2-5 outline the use of these ligands in the formation of manganese(II), nickel(II) and zinc(II) complexes, the structural assignments of which are based on a consideration of the microanalysis and infrared data.

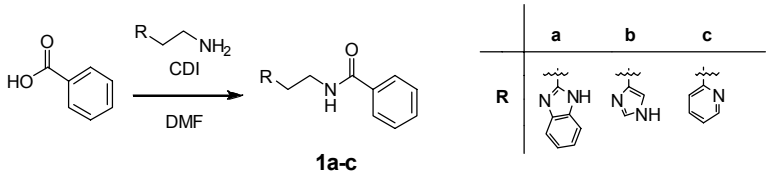

Scheme 1. Synthesis of benzamide-derived ligands.

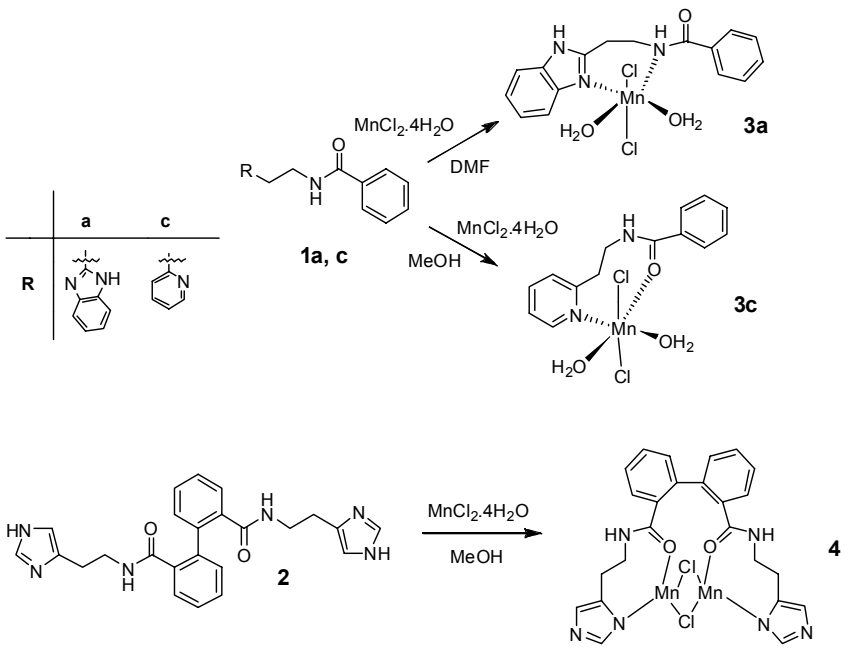

Scheme 2. Manganese(II) complexes of the benzamide- and biphenyl-derived ligands.

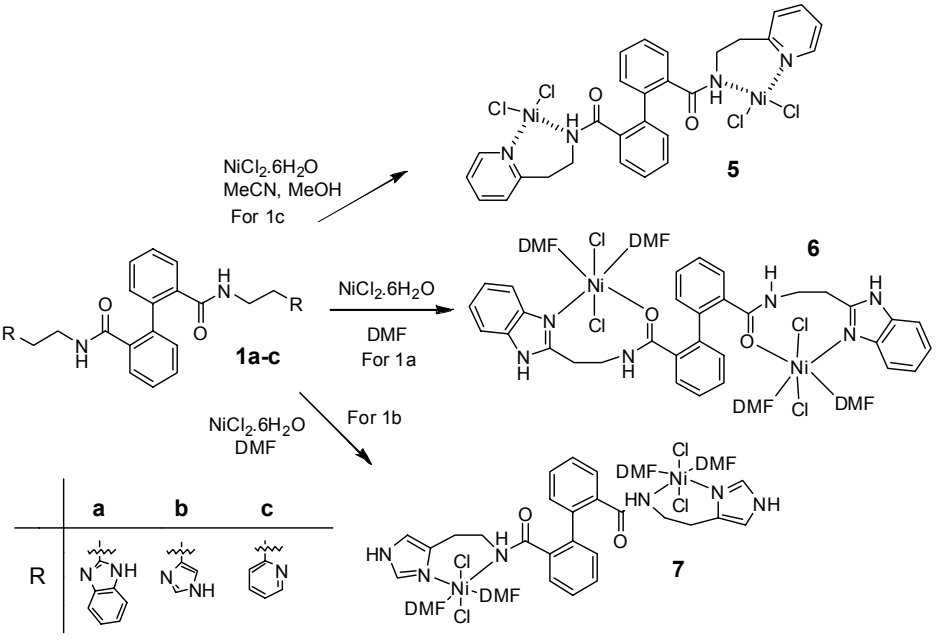

Scheme 3. Nickel(II) complexes of the biphenyl-derived ligands.

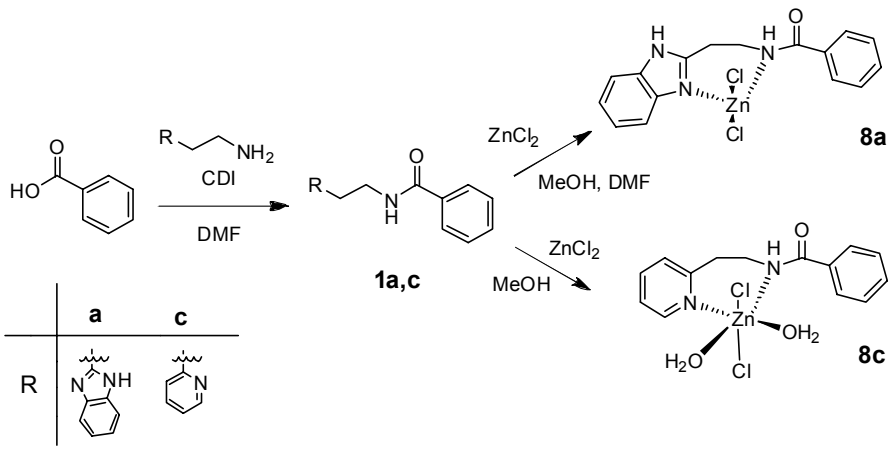

Scheme 4. Zinc(II) complexes of the benzamide-derived ligands.

Microanalysis data for the various complexes are summarized in Table 1. It is apparent that the manganese complexes **3a** and **3c** are mononuclear while complex **4** is dinuclear; all three complexes, however, contain two chloride ions (Scheme 2). The nickel complexes **5-7** (Scheme 3) all appear to be dinuclear and each complex contains four chloride ions. The diamide- and monoamide zinc complexes [**8a,c** and **9a-c,** respectively (Schemes 4 and 5)] all appear to be mononuclear and contain only two chloride ions. The structures proposed for the various complexes (Schemes 2-5) are consistent with the microanalysis and corresponding infrared data (Table 2).

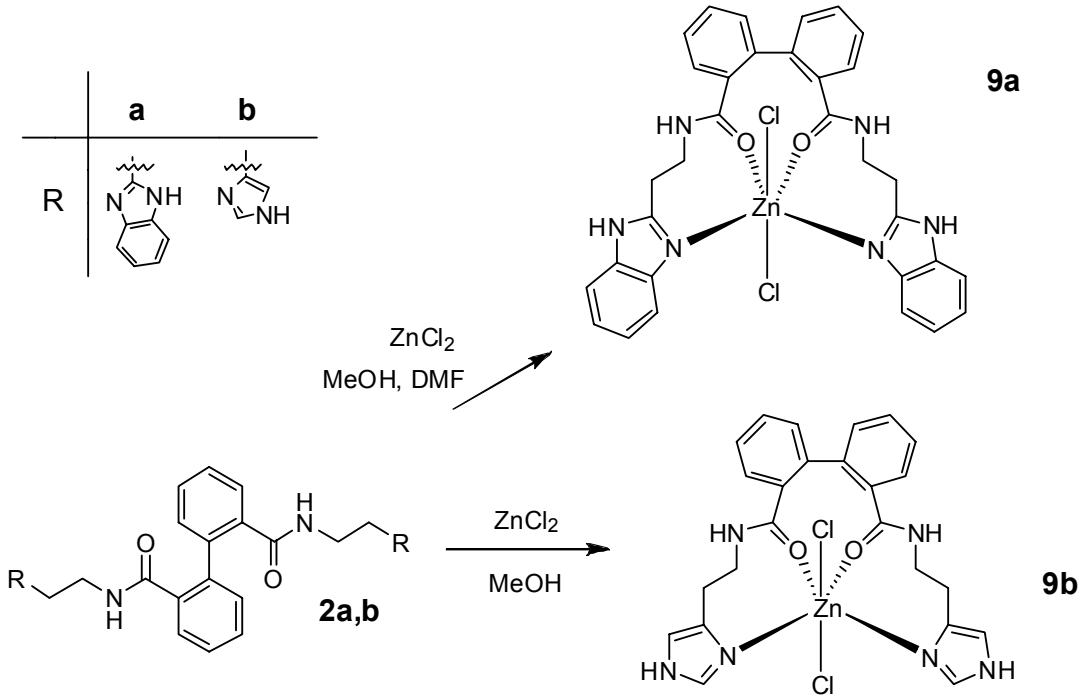

Scheme 5. Zinc(II) complexes of the biphenyl-derived ligands.

Table 1. Microanalytical data for the metal complexes followed, in parentheses, by the calculated values

Complex	Complex Stoichiometry[a]	% Carbon	% Hydrogen	% Nitrogen
3a	Mn(**1a**)Cl_2.2H_2O	44.7 (45.0)	4.5 (4.5)	9.6 (9.8)
3c	Mn(**1c**)Cl_2.2½H_2O	42.6 (42.3)	4.2 (4.3)	7.1 (7.1)
4	Mn_2(**2**)Cl_2	47.8 (47.5)	3.5 (3.7)	13.5 (13.8)
5	Ni_2(**1c**)Cl_4.6H_2O	40.5 (41.1)	4.2 (4.7)	7.0 (6.9)
6	Ni_2(**1a**)Cl_2.$(DMF)_4$	39.4 (38.9)	3.3 (3.8)	9.5 (9.1)
7	Ni_2(**1b**)Cl_2.$(DMF)_4$.3H_2O	41.4 (41.8)	5.2 (5.7)	13.2 (13.5)
11	Ni(**10**)Cl_2.1H_2O	57.1 (56.5)	4.6 (5.0)	6.7 (6.3)
8a	Zn(**1a**)Cl_2.DMF	48.3 (48.1)	4.6 (4.7)	11.4 (11.8)
8c	Zn(**1c**)Cl_2.3H_2O	40.4 (40.5)	4.3 (4.6)	6.8 (6.7)
9a	Zn(**2a**)Cl_2.3H_2O	51.2 (50.9)	4.9 (4.6)	11.4 (11.1)
9b	Zn(**2b**)Cl_2.2H_2O	47.9 (48.0)	4.7 (4.7)	13.8 (14.0)

[a] Presence of H_2O and/or DMF supported by IR data; see Table 2 for $\nu(OH_2)$ data.

Mid-IR spectra of the complexes were used to establish whether the manganese ions coordinate through the amide nitrogen or oxygen atoms, while the environment of the coordinated chloride anions was determined by running spectra in the far-IR region. Both negative and positive shifts may be observed for the amide carbonyl band (amide I) − a negative shift indicating coordination *via* the amide oxygen, a positive shift coordination *via* the amide nitrogen. For the manganese monoamide complex **3a**, the absence of any significant change in $\nu_{C=O}$ coupled with a small positive shift (16 cm^{-1}) of the benzamide NH band (relative to the free ligand) indicates coordination *via* the amide nitrogen, while the presence of the benzimidazole NH indicates coordination with the tertiary benzimidazole nitrogen. In the case of the pyridyl analogue **3c** and the diamide complex **4**, the significant positive amide NH band shifts, coupled with the negative C=O band shifts, are consistent with coordination *via* the amide carbonyl oxygen. The far-IR bands at 278 and 276 cm^{-1} are consistent with chloride ions in an octahedral environment in complexes **3a** and **3c**, respectively; the two, lower-frequency bands at 217 and 271 cm^{-1} for complex **4** are characteristic of chloride bridging.[17]

Coordination of nickel through the amide oxygen in the diamide complex **6** is indicated by the small positive NH and negative C=O shifts. In complexes **5** and **7**, coordination through the amide nitrogen is suggested by the positive amide NH shifts; complex **7** also exhibits a positive carbonyl shift, but complex **5** none. The presence of the amide NH band in all cases implies that deprotonation of the amide nitrogen has not occurred − an observation consistent with the microanalysis data for these nickel complexes. Very weak bands at 276 and 325 cm^{-1} in the far IR region were observed for complex **5** and are attributed to Ni-Cl stretches in a square planar environment. In the case of complexes **6** and **7** the strong bands in the 370-390 cm^{-1} region are

attributed to chloride anions coordinated in a *trans* octahedral geometry.[17] The X-ray crystal structure for complex **11** (Scheme 6 and Figure 1) clearly confirms the tetrahedral geometry responsible for the two relatively strong bands at 289 and 329 cm^{-1}; these values are characteristic of chloride ions coordinated in a tetrahedral environment[17] − in contrast with the somewhat lower values attributed to the square-planar complex **5**.

Table 2. Summary of the IR frequencies (V_{M-Cl}) and the amide frequency shifts (ΔV_{NH} and $\Delta V_{C=O}$) on formation of the metal complexes

Complex	$\Delta\nu_{NH}/cm^{-1}$	$\Delta\nu_{C=O}/cm^{-1}$	ν_{M-Cl}/cm^{-1}	ν_{OH}[a]$/cm^{-1}$
3a	16	1	278	3500
3c	54	-4	276	3400
4	42	-21	217, 271	-
5	15[b]	0[b]	276, 325	3375[b]
6	11	-6	387	3321
7	49	13	378	3400
8a	16	31	287	-
8c	101[c,d]	0[c]	278	3496[c]
9a	50	-8	278	3420 (sh)
9b	83	10	281	3520 (sh)

[a] Broad H_2O bands. [b] In HCBD. [c] In NaCl. [d] Shoulder.

For complex **8a**, the small positive shifts of both the amide carbonyl and amide NH bands indicate coordination through the amide nitrogen (the apparent broadening of the amide carbonyl band is attributed to the presence of DMF). In complex **8c**, no shift of the amide carbonyl band is evident and the large positive shift (*ca*. 100 cm^{-1}) of the amide NH band points to coordination with the amide nitrogen. The negative shift of the amide CO band in complexes **9a** and **9b** is an indication that coordination occurs with the amide oxygen atom. From the data in Table 2 it appears that the amide functionality in these complexes is resistant to deprotonation. Two Zn-Cl bands characteristic of tetrahedral geometry are anticipated in the far-lR region (*ca*. 295 and 327 cm^{-1}) for complex **8a**, but this was not observed.[17] Instead, a very strong, broad band, with shoulders, is observed at *ca*. 287 cm^{-1}. This band may reflect accidental degeneracy of the symmetric and anti-symmetric Zn-Cl stretches due to a distorted tetrahedral zinc arrangement within this complex. The mononuclear zinc complexes **9a** and **9b** exhibit less intense bands at lower wave-numbers in the far-IR region and these are attributed to Zn-Cl stretches in an octahedral arrangement.[17]

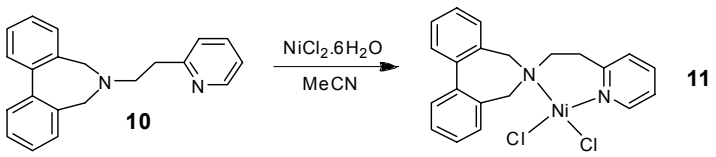

Scheme 6

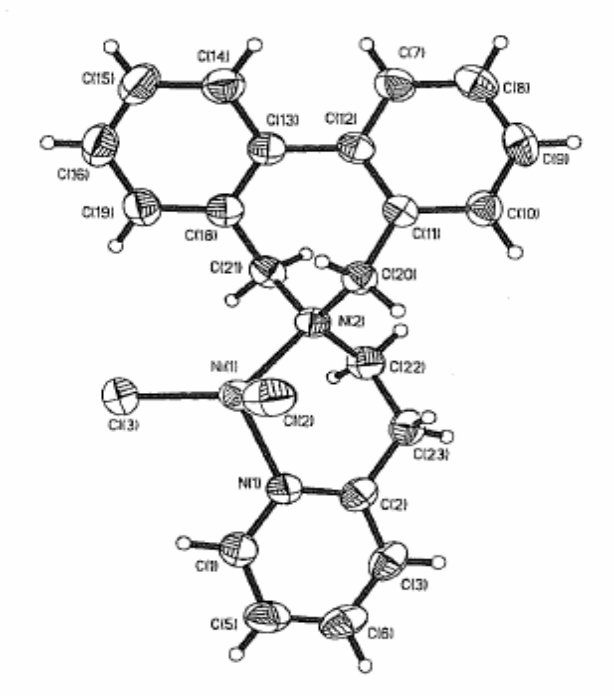

Figure 1. X-ray crystal structure of complex **11** showing the crystallographic numbering.

NMR analysis (^{1}H, ^{13}C and DEPT 135) of the zinc(II) complexes revealed broadening of the ligand signals − a phenomenon observed in other studies[18] and attributed to site-exchange processes involving coordination to the metal centre. Signal broadening is particularly marked in the ^{1}H NMR spectrum of complex **9b**, while the corresponding ^{13}C spectrum reveals doubling of certain ligand signals, consistent with slow (on the NMR time-scale) site-exchange between non-equivalent structural arrangements. In the case of complex **8c**, on the other hand, only slight broadening of the ^{1}H signals is apparent.

The phenolase and catecholase activity of the manganese(II) complexes were investigated to determine whether these complexes are capable of mimicking the active site of the enzyme tyrosinase. This was investigated because manganese is a redox metal and capable of binding oxygen - as can be seen in the formation of the complexes **3c** and **4**. In order to evaluate the 'phenolase' and 'catecholase' activity of the complexes, 3,5-di-*t*-butylphenol (3,5-DTBP) and 3,5-di-*t*-butylcatechol (3,5-DTBC) were used as the respective substrates.[19-21] [3,5-DTBP is

oxidized to 3,5-DTBC, which is oxidized, in turn, to 3,5-di-*t*-butyl-*o*-quinone (3,5-DTBQ); if formed, the oxidation products may be readily detected by ^{1}H-NMR analysis].

Table 3. Catecholase activity of the manganese(II) complexes

Complex	Solvent	Reaction Time/h	Phenolase Activity Product	Catecholase Activity Product	% Conversion within 24 h	Recyclability: % coversion within 24 h
3a	DMF	24	-	*o*-quinone	100	100
3c	DMF	24	-	*o*-quinone	75	-
4	DMF	24	-	*o*-quinone	100	100

It can be seen from the data summarised in Table 3 that while no phenolase activity was observed, catecholase activity was exhibited by the three manganese complexes **3a**, **3c** and **4**. Phenolase activity requires initial *axial* binding of the phenol to the metal centre, followed by Berry pseudorotation of the trigonal bipyramidal complex, to expose the *equatorial* substrate to *ortho*-hydroxylation. This may be inhibited in these complexes and, as a consequence, no phenolase activity was observed. Catecholase activity is easier to achieve since it only requires a transfer of electrons and it is observed for complexes **3a**, **3c** and **4**. The catecholase activities of the mangananese complexes complexes **3a** and **4** are greater than those exhibited by our biphenyl dinuclear cobalt(II) complexes ($\leq$ 88%)[5] and by our macrocyclic dinuclear copper(I) and copper(II) complexes (63% and 83% conversion, respectively), but comparable with the activity of our macrocyclic dinuclear cobalt(II) complex (100% conversion).[22] The catalytic oxidation of 3,5-DTBC to 3,5-DTBQ by a series of mononuclear manganese complexes has been reported previously,[23] and our results are similar to those observed for [M^{II}(diclofenac)$_2$H$_2$O)] complexes (M = Mn, Co, Ni, Cu).[24]

Conclusions

It is apparent that the benzamide- and biphenyl-derived ligands examined here form complexes with manganese(II), nickel(II) and zinc(II) and that, depending on the ligand, the metal centres in these complexes adopt octahedral, tetrahedral or distorted tetrahedral coordination geometries. The structures of the complexes have been assigned using elemental analysis data, mid- and far-infrared and, where appropriate, NMR spectroscopic data. Significant catecholase activity (75 – 100% conversion within 24 hours) has been demonstrated for the manganese(II) complexes **3a**, **3c** and **4**, while complexes **3a** and **4** also exhibit encouraging recyclability (100% conversion within 24 hours).

Table 4. Atomic coordinates (x 10^4) for complex **11** and equivalent isotropic displacement parameters ($Å^2$ x 10^3) U(eq) is defined as one third of the trace of the orthogonalized Uij tensor

	x	y	z	U(eq)
Ni (1)	2197 (1)	1086 (1)	2108 (1)	41 (1)
Cl (1)	3094 (1)	1985 (1)	3225 (1)	68 (1)
N (1)	4142 (3)	589 (2)	1657 (2)	39 (1)
C (1)	5243 (4)	1134 (2)	1417 (3)	46 (1)
Cl (2)	861 (1)	1315 (1)	718 (1)	56 (1)
C (2)	6558 (4)	879 (3)	991 (3)	51 (1)
N (2)	1270 (3)	46 (2)	2744 (2)	33 (1)
C (3)	6770 (4)	38 (3)	816 (2)	50 (1)
C (4)	5679 (4)	-526 (2)	1082 (2)	46 (1)
C (5)	4344 (4)	-239 (2)	1499 (2)	40 (1)
C (6)	3092 (4)	-831 (2)	1754 (3)	48 (1)
C (7)	2390 (4)	-671 (2)	2734 (2)	42 (1)
C (8)	-192 (3)	-185 (2)	2207 (2)	35 (1)
C (9)	-1226 (3)	-791 (2)	2711 (2)	34 (1)
C (10)	-1432 (4)	-1611 (2)	2366 (2)	42 (1)
C (11)	-2527 (4)	-2130 (2)	2755 (3)	51 (1)
C (12)	-3421 (4)	-1840 (2)	3487 (3)	53 (1)
C (13)	-3223 (4)	-1030 (2)	3839 (3)	47 (1)
C (14)	-2125 (3)	-493 (2)	3459 (2)	36 (1)
C (15)	-1930 (3)	380 (2)	3839 (2)	37 (1)
C (16)	-3192 (4)	858 (2)	4095 (3)	48 (1)
C (17)	-3015 (5)	1644 (2)	4514 (3)	55 (1)
C (18)	-1582 (5)	1973 (2)	4668 (3)	55 (1)
C (19)	-317 (4)	1528 (2)	4391 (2)	47 (1)
C (20)	-465 (4)	728 (2)	3968 (2)	38 (1)
C (21)	932 (4)	202 (2)	3792 (2)	37 (1)

Table 5. Bond lengths (in Angstroms) with standard deviations for complex **11**

Ni(1)-N(1)	1.997 (2)
Ni (1)-N(2)	2.047 (2)
Ni (1)-C (1)	2.2229 (11)
Ni (1)-C (2)	2.2447 (10)
N(1)-C(S)	1. 342 (4)
N(1)-C(1)	1.344 (4)
C(1)-C(2)	1.372 (5)
C(2)-C(3)	1.368 (5)

N(2)-C(7)	1.501 (4)
N(2)-C(8)	1.505 (4)
N(2)-C(21)	1.506 (4)
C(3)-C(4)	1. 368 (5)
C(4)-C(5)	1.397 (4)
C(5)-C(6)	1.495 (5)
C(6)-C(7)	1.525 (5)
C(8)-C(9)	1.506 (4)
C(9)-C(10)	1.393 (4)
C(9)-C(14)	1.401 (4)
C(10)-C(11)	1.386 (5)
C(11)-C(12)	1.377 (5)
C(12)-C(13)	1. 381 (5)
C(13)-C(14)	1.399 (4)
C(14)-C(15)	1.487 (4)
C(15)-C(16)	1.395 (4)
C(15)-C(20)	1. 403 (4)
C(16)-C(17)	1.380 (5)
C(17)-C(18)	1.370 (6)
C(18)-C(19)	1. 379 (5)
C(19)-C(20)	1.400 (5)
C(20)-C(21)	1.508 (4)

Table 6. Bond angles [deg] for complex **11**

N(1)-Ni(1)-N(2)	99.87 (10)
N(1)-Ni(1)-C1(1)	100.49 (8)
N(2)-Ni(1)-C1(1)	110.81 (7)
N(1)-Ni(1)-C1(2)	102.97 (8)
N(2)-Ni(1)-C1(2)	107.03 (7)
C1(1)-Ni(1)-Cl(2)	130.68 (4)
C(5)-N(1)-C(1)	119.2 (3)
C(5)-N(1)-Ni(1)	123.7 (2)
C(1)-N(1)-Ni(1)	116.8 (2)
N(1)-C(1)-C(2)	122.5 (3)
C(3)-C(2)-C(1)	118.9 (4)
C(7)-N(2)-C(8)	111.1 (2)
C(7)-N(2)-C(21)	106.4 (2)
C(8)-N(2)-C(21)	108. 8 (2)
C(7)-N(2)-Ni(1)	109.6 (2)
C(8)-N(2)-Ni(1)	109.2 (2)

C(21)-N(2)-Ni(1)	111.8 (2)
C(4)-C(3)-C(2)	119.2 (3)
C(3)-C(4)-C(5)	120.0 (3)
N(1)-C(5)-C(4)	120.1 (3)
N(1)-C(5)-C(6)	118.3 (3)
C(4)-C(5)-C(6)	121.6 (3)
C(S)-C(6)-C(7)	115.1 (3)
N(2)-C(7)-C(6)	114.6 (3)
N(2)-C(8)-C(9)	116.3 (2)
C(10)-C(9)-C(14)	119.7 (3)
C(10)-C(9)-C(8)	120.6 (3)
C(14)-C(9)-C(8)	119.2 (3)
C(11)-C(10)-C(9)	120.3 (3)
C(12)-C(11)-C(10)	120.3 (3)
C(11)-C(12)-C(13)	120.0 (3)
C(12)-C(13)-C(14)	120.9 (3)
C(13)-C(14)-C(9)	118.8 (3)
C(13)-C(14)-C(15)	120.4 (3)
C(9)-C(14)-C(15)	120.8 (3)
C(16)-C(15)-C(20)	119.0 (3)
C(16)-C(15)-C(14)	120.7 (3)
C(20)-C(15)-C(14)	120.2 (3)
C(17)-C(16)-C(15)	121.1 (4)
C(18)-C(17)-C(16)	119.9 (4)
C(17)-C(18)-C(19)	120.3 (4)
C(18)-C(19)-C(20)	120.9 (3)
C(19)-C(20)-C(15)	118.7 (3)
C(19)-C(20)-C(21)	120.2 (3)
C(15)-C(20)-C(21)	120.6 (3)
N(2)-C(21)-C(20)	115.6 (2)

Experimental Section

General Procedures. Infrared spectra were recorded on a Perkin Elmer 2000 spectrophotometer using potassium bromide discs (4000–400 cm^{-1}), hexachlorobutadiene mulls (HCBD; 4000–2000 and 1500–1250 cm^{-1}), polyethylene discs (500–30 cm^{-1}) or nujol mulls (500–30 cm^{-1}). Infrared spectra were recorded on a Perkin Elmer 2000 spectrophotometer using potassium bromide discs (4000-400 cm and nujol mulls (650 - 30 cm^{-1}) NMR spectra were recorded on a Bruker AMX 400 spectrometer and chemical shifts are reported relative to the solvent peaks.

Low resolution mass spectra were obtained on a Hewlett-Packard 5988A mass spectrometer, and high resolution analyses on a Kratos MS8ORF double focussing magnetic sector instrument (Cape Technikon Mass spectrometry unit). Microanalysis (combustion analysis) was conducted at the University of Cape Town, and the data for the zinc complexes are reported in Table 1. Melting points were obtained using a Kofler hot-stage microscope and are uncorrected.

***N*-[(2-Benzimidazolyl)ethyl]benzamide (1a)**

Benzoic acid (1.00 g, 8.19 mmol) was dissolved in dry DMF (10 mL) in a round- bottomed flask fitted with a reflux condenser and drying tube. The solution was warmed to 40°C, and CDI (2.16 g, 13.32 mmol) was added with stirring. The mixture was stirred for 5 min at 40°C, after which time, gas evolution ceased. After cooling to room temperature, 2-(2-aminoethyl)benzimidazole (1.32 g, 8.19 mmol) was added. The resulting solution was stirred for 60 h at room temperature, and the reaction was quenched with H_2O (7 mL). The pale pink powder that precipitated was filtered off and washed with aqueous Na_2CO_3 (1M; 50 mL) to give *N*-[(2-benzimidazolyl)ethyl]-benzamide **1a** (1.58 g, 73%), mp >250°C[25] (from DMF-H_2O (Found: **MH**$^+$266.1294. $C_{16}H_{15}N_3O$ requires, *MH* 266.1293); ν_{max}(KBr/cm^{-1}, 3305 (amide NH), 3176 (benzimidazole NH),1638 (CO); δ_H(400 MHz; DMSO-d_6) 3.09 (2H, t, $NHCH_2$ CH_2), 3.73 (2H, m, $NHCH_2CH_2$), 7.12 (2H, m, ArH), 7.49 (5H, m, ArH), 7.84(2H, d, ArH), 8.63 (1H, m, amide NH), 12.50 (1H, s, NH); δ_c(100 MHz; DMSO-d_6) 28.8 (t, $NHCH_2CH_2$), 38.0 (t, $NHCH_2CH_2$), 110.8(d), 118.1(d), 120.8(d), 121.5(d), 127.1(d), 128.2(d), 131.1(d), 134.2(s), 134.4(s), 143.2(s) and 152.8(s) (ArC) and 166.2 (s, CO).

***N*-[(2-Imidazolyl)ethyl]benzamide (1b)**

Benzoic acid (1.00 g, 8.19 mmol) was dissolved in dry DMF (10 mL) in a round-bottomed flask fitted with a reflux condenser and drying tube. The solution was warmed to 40°C, and CDI (2.16 g, 13.32 mmol) was added with stirring. The mixture was stirred for 5 min at 40°C, after which time, gas evolution ceased. After cooling to room temperature, histamine (0.92 g, 8.19 mmol) was added. The resulting solution was stirred for 46 h at room temperature, and the reaction was quenched with H_2O (7 mL). Volatiles were removed under reduced pressure and aqueous 1 M Na_2CO_3 (50 mL) was added. The mixture was extracted with EtOAc (4 x 100 mL), and the combined extracts were washed with H_2O (100 mL) and brine (100 mL), and dried ($MgSO_4$). The solvent was evaporated to afford, as a yellow solid, *N*-[(2-imidazolyl)ethyl]benzamide **1b** (1.74 g, 99%), mp 149-150°C (from MeOH-H_2O) (Lit.[26] 145-148°C) (Found: **MH**$^+$ 215.1050. $C_{16}H_{15}N_3O$ requires, *MH* 215.1059); ν_{max} (KBr/cm^{-1}) 3223 (amide NH), 3152 (imidazole NH) and 1634 (CO); δ_H(400 MHz; DMSO-d_6) 2.77 (2H, t, $NHCH_2CH_2$), 3.45-3.53 (2H, m, $NHCH_2CH_2$), 6.82 (1H, s, ArH), 7.45 (2H, t, ArH), 7.48-7.55 (2H, m, ArH), 7.83 (2H, d, ArH), 8.53 (1H, m, amide NH), 11.82 (1N, s, NH).

***N*-[(2-Pyridinyl)ethyl]benzamide (1c)**

Following the procedure used for the preparation of *N*-[(2-benzimidazolyl)ethyl]-benzamide **1a**, benzoic acid (1.00 g, 8.19 mmol), CDI (2.16 g, 13.32 mmol) and 2-(2-aminoethyl)pyridine (0.98 mL, 8.19 mmol) in dry DMF (10 mL) was stirred for 72 h at room temperature before quenching

with H_2O (7 mL). Volatiles were removed under reduced pressure, and aqueous 1 M Na_2CO_3 (50 mL) was added to the residual oil. The mixture was extracted with EtOAc (4 x 100 mL), and the combined extracts were washed with H_2O (100 mL) and brine (100 mL), and dried ($MgSO_4$). The solvent was evaporated and the residue chromatographed [chromatography on silica gel; elution with $CHCI_3$ (1:3:3)] to afford, as a white crystalline solid, *N*-[(2-pyridinyl)ethyl]benzamide **1c** (1.61 g, 87%), mp 68-69°C (Lit.[27] 68-70°C) (Found: $\mathbf{M}^+$ 226.1097. $C_{28}H_{26}O_2N_4$ requires, *M* 226.1107); v_{max}(KBr/cm^{-1}) 3290 (amide NH) and 1627 (CO); δ_H(400 MHz; DMSO-d_6) 3.01 (2H, t, $NHCH_2CH_2$), 3.59-3.67 (2H, m, $NHCH_2CH_2$), 6.85-7.23 (2H, m, ArH), 7.27 (2H, d, ArH), 7.41 -7.47 (4H, m, ArH), 7.48-7.52 (2H, m, ArH), 7.67-7.72 (2H, m, ArH), 7.79-7.85 (4H, m, ArH), 8.49-8.52 (2H, m, ArH), 8.53 (1 H, m, amide NH); δ_c(100 MHz; DMSO-d_6) 37.2 (t, $NHCH_2CH_2$), 39.1 (t, $NHCH_2CH_2$), 121.4(d), 123.0(d), 127.0(d), 128.1(d), 130.9(d), 134.5(s), 136.3(d), 149.0(d), 159.3(s) (ArC) and 166.0 (s, CO).

The manganese complex 3a

A hot solution of *N*-[(2-benzimidazolyl)ethyl]benzamide **1a** (0.15 g, 0.57 mmol) in DMF (13 mL) was added dropwise to a solution of $MnCl_2.4H_2O$ (0.11 g, 0.57 mmol) in DMF (2 mL), and the reaction mixture was stirred for 60 h. The solvent was evaporated off under reduced pressure, re-dissolved in DMF, and Et_2O and hexane added to precipitate, as a light-brown solid, the *manganese complex* **3a** (0.14 g, 57%), mp 189-192°C; v_{max}(KBr/cm^{-1}) 3321 (amide NH), 3200 (benzimidazole NH) and 1639 (CO); v_{max}(nujol/cm^{-1}) 278 (Mn-Cl).

The manganese complex 3c

To a stirred solution of *N*-[(2-pyridinyl)ethyl]benzamide **1c** (0.17 g, 0.75 mmol) in MeOH (3 mL), a solution of $MnCl_2.4H_2O$ (0.17 g, 0.75 mmol) in MeOH (5 mL) was added and the reaction mixture stirred for 53 h. The solvent was removed under reduced pressure to less than half the original volume before adding Et_2O to precipitate the product. The residual oil that precipitated was washed with Et_2O followed by drying under vacuum to afford, as a light-brown powder, the *manganese complex* **3c**, (0.29 g, 97%), mp 103-105°C; v_{max}(KBr/cm^{-1}) 3344 (amide NH) and 1623 (CO); v_{max}(nujol/cm^{-1}) 276 (Mn-Cl).

The manganese complex 4

A solution of 2,2'-bis{[2-(4-imidazolyl)ethylamino]carbonyl}biphenyl **2b** (0.20 g, 0.46 mmol) in MeOH (9 mL) was added to a stirred solution of $MnCl_2.4H_2O$ (0.18 g, 0.92 mmol) in MeOH (3 mL). After stirring for 39 h, Et_2O was added to precipitate the product. The *manganese complex* **4** was obtained as a cream powder after recrystallising from MeOH-Et_2O (0.20 g, 72%), mp 205-207°C; v_{max}(KBr/cm^{-1}) 3237 (amide NH), 3137 (imidazole NH) and 1630 (CO); v_{max}(nujol/cm^{-1}) 271 and 217 (Mn-Cl).

The nickel complex 5

A solution of 2,2'-bis{[2-(2-pyridyl)ethylamino]carbonyl}biphenyl **2c** (0.20 g, 0.44 mmol) in MeOH (5 mL) was added to a stirred solution of $NiCl_2.6H_2O$ (0.22 g, 0.92 mmol) in MeCN (5 mL). After stirring for 2.5 d, Et_2O was added to precipitate, as a light-green, hygroscopic solid, *the nickel complex* **5** (0.26 g, 72%), mp 48-49°C;
v_{max}(KBr/cm^{-1}) 3336 (amide NH) and 1619 (CO); v_{max}(nujol/cm^{-1}) 325 and 276 (Ni-Cl).

The nickel complex 6

A hot solution of 2,2'-bis{[2-(2-benzimidazolyl)ethylamino]carbonyl}biphenyl **2a** (0.23 g, 0.44 mmol) was added dropwise to a stirred solution of $NiCl_2.6H_2O$ (0.22 g, 0.92 mmol) in DMF (7 mL). The reaction mixture was stirred for 57 h before Et_2O was added to precipitate, as a light-green solid, *the nickel complex* **6** (0.29 g, 53%), mp >250°C; ν_{max} (KBr/cm^{-1}) 3183 (amide NH) and 1650 (CO); ν_{max}(nujol/cm^{-1}) 387 (Ni-Cl).

The nickel complex 7

A solution of 2,2'-bis{[2-(4-imidazolyl)ethylamino]carbonyl}biphenyl **2b** (0.15 g, 0.35 mmol) in DMF (10 mL) was added dropwise to a stirred solution of $NiCl_2.6H_2O$ (0.17 g, 0.72 mmol) in MeOH (5 mL). Stirring was continued for 55 h before adding Et_2O to precipitate, as a hygroscopic dark blue-green solid, *the nickel complex* **7***,* (0.10 g, 27%), mp 204-205°C; ν_{max}(KBr/cm^{-1}) 3248 (amide NH), 3143 (imidazole NH) and 1653 (CO); ν_{max}(nujol/cm^{-1}) 378 (Ni-Cl).

The nickel complex 11

To a stirred solution of $NiCl_2.6H_2O$ (0.22 g, 0.92 mmol) in MeOH (4 mL), a solution of 1-[2-(2-pyridyl)ethyl]dibenz[*c,e*]perhydroazepine **10**[28] (0.19 g, 0.44 mmol) in MeCN (10 mL) was added dropwise, and stirring was continued for 19 h. The solvent was allowed to evaporate off at room temperature, during which time, purple crystals precipitated from the reaction mixture and were filtered off to give *the nickel complex* **11** (0.13 g, 65%), mp >250°C; ν_{max}(nujol/cm^{-1}) 329 and 289 (Ni-Cl).

The zinc complex 8a

A solution of N-*[(2-benzimidazolyl)ethyl]benzamide* **1a** (0.15 g, 0.57 mmol) in hot DMF (6 mL) was added dropwise to a solution of $ZnCl_2$ (0.08 g, 0.57 mmol) in a mixture of MeOH (4 mL) and DMF (4 mL), and the reaction mixture was stirred for 48 h. The solvent was evaporated off under reduced pressure, re-dissolved in DMF, and Et_2O and hexane added to precipitate, as a light-brown solid, the *zinc complex* **8a** (0.23 g, 85%), mp >96-98°C; ν_{max}(KBr/cm^{-1}) 3321 (amide NH), 3183 (imidazole NH) and 1646 (CO); ν_{max}(nujol/ cm^{-1}) 287 (Zn-Cl); δ_H(400 MHz; DMSO-d_6) 3.23 (2H, m, CH_2), 3.72 (2H, m, CH_2N), 7.24 (2H, br s, ArH), 7.44 (2H, t, ArH), 7.51 (1H,t, ArH), 7.70 (2H, br s, ArH), 7.82 (2H, d, ArH), 7.95 (1H s, NH) and 13.10 (1H, br s, NH); δ_c(100 MHz; DMSO-d_6) 28.4 (t, CH_2), 38.8 (t, CH_2N), 122.3 (d), 127.1 (d), 128.1 (d), 131.0 (d), 134.3 (s), 154.3 (s) and 162.2 (d) (ArC) and 166.4 (s, C=O).

The zinc complex 8c

To a stirred solution of N-*pyridinyl)ethyl]benzamide* **1c** (0.17 g, 0.75 mmol) in MeOH (3 mL), a solution of $ZnCl_2$ (0.17 g, 0.75 mmol) in MeOH (5 mL) was added and the reaction mixture stirred for 53 h. The solvent was removed under reduced pressure and the residue washed with Et_2O to afford, as a yellow-white semi-solid, the *zinc complex* **8c**, (0.29 g, 97%); ν_{max}(KBr/cm^{-1}) 3496 (amide NH) and 1627 (CO); ν_{max}(nujol/ cm^{-1}) 278 (Zn-Cl); δ_H(400 MHz; DMSO-d_6) 3.01 (2H, t, CH_2), 3.62 (2H, q, CH_2N), 7.22 (1H, t, ArH), 7.28 (1H, d,ArH), 7.44 (2H, t, ArH), 7.50 (1H, t, ArH), 7.70 (1H, t, ArH), 7.80 (2H, d, ArH), 8.51 (1H, d, ArH) and 8.56 (1H, m, NH);

δ_c(100 MHz; DMSO-*d*$_6$) 37.2 (t, CH_2), 39.2 (t, CH_2N), 121.5 (d), 123.1 (d), 127.0 (d), 128.2 (d), 131.0 (d), 134.5 (s), 136.5 (d), 149.0 (d) and 159.1 (s) (ArC) and 166.0 (s, C=O).

The zinc complex 9a

A hot, clear, colourless solution of 2,2'-bis{[2-*(2-benzimidazolyl)ethylamino]carbonyl}-biphenyl* **2a** (0.25 g, 0.47 mmol) in DMF (40 mL) was added to a stirred solution of $ZnCl_2$ (0.13 g, 0.95 mmol) in DMF (5 mL) and MeOH (5 mL). After stirring for 68 h Et was added to precipitate the product. Recrystallisation from DMF-Et_2O yielded, as a cream-white solid, the *zinc complex* **9a** (0.22 g, 62%), mp >250°C; ν_{max}(KBr/cm^{-1}) 3255 (amide NH), 3152 (imidazole NH) and 1648 (CO); ν_{max}(nujol/cm^{-1}) 278 (Zn-Cl); δ_H(400 MHz; DMSO-*d*$_6$) 2.85 (2H, br s, CH_2), 3.40 [2H, m(sh), CH_2N], 6.96-8.69 (9H, series of br s, ArH and NH) and 12.70 (1H, br s, NH); δ_c(100 MHz; DMSO-*d*$_6$) 28.0 (t, CH_2), 37.2 (t, CH_2N), 111.2 (br s), 121.9 (br d), 127.2 (d), 128.9 (d), 129.1 (d), 135.6 (s), 138.9 (s), 153.6 (s) and 162.2 (s) (ArC) and 169.0 (s, C=O).

The zinc complex 9b

A solution of 2,2'-bis{[2-*(4-imidazolyl)ethylamino]carbonyl}biphenyl* **2b** (0.24 g, 0.56 mmol) in MeOH (20 mL) was added to a stirred solution of $ZnCl_2$ (0.15 g, 1.1 mmol) in MeOH (6 mL). After stirring for 48 h, Et_2O was added to precipitate the product. The *zinc complex* **6a** was obtained as a cream-white powder after recrystallising from MeOH-Et_2O (0.15g, 45%), mp >219-221°C; ν_{max}(KBr/cm^{-1}) 3237 (amide NH), 3137 (imidazole NH) and 1630 (CO); ν_{max}(nujol/cm^{-1}) 281 (Zn-Cl); δ_H(400 MHz; DMSO-*d*$_6$) 1.8-3.9 (4H, series of br s, CH_2CH_2N), 6.85 (1H, br s, ArH), 6.89 (1H, d, ArH), 7.36 (3H, br s, ArH), 7.97 (1H, br s, ArH), 8.60 (1H, br d, ArH) and 12.8 (1H, br d, NH); δ_c(100 MHz; DMSO-*d*$_6$) 25.3/25.7* (t, CH_2), 36.7/37.6* (t, CH_2N), 114.0, 123.4, 127.4, 128.3, 128.9/129.2 and 136.3 (6 x d, ArC), 134.5, 139.0 and 139.4 (3 x s, ArC) and 168.4/169.2* (s, C=O).

X-Ray crystal data for complex 11. $C_{21}H_{20}Cl_2N_2Ni$, M = 430; monoclinic, space group P2(1)/n; a = 8.7689 (5), b = 15.8377 (9), c = 13.7979 (8) Å, α = 90.00°; β = 91.8760° (10); γ = 90.00°, V = 1915.2(2) Å^3, Z = 4, F(000) = 888, D_c = 1.491 gcm^{-3}, μ = 1.299 mm^{-1}. Data collection with graphite-monochromated Mo-K_α radiation, λ = 0.71073 Δ, T = 296(2) K, θ range 1.96 to 28.28E, 11748 reflections collected (- 11 < h < 10, - 20 < k < 20, - 17 < l < 16), 4317 unique with I > 2σ(I). Hydrogen atoms were placed in calculated positions and the structure was solved by direct methods using SHELX-97;[29] full-matrix least-squares refinement converged at R_1 = 0.0494, wR_2 = 0.0979, GOF = 1.132. CCDC 704606 contains the supplementary crystallographic data for this paper. These data can be obtained free of charge from The Cambridge Crystallographic Data Centre *via* www.ccdc.cam.ac.uk/data_request/cif

Catalytic studies

The substrates 3,5-DTBP (100 eq.) and 3,5-DTBC (100 eq.) were added to solutions of the Mn(II) complexes (0.01g) in DMF (2 mL for **3a**, **4**; 2.5 mL for **3c**), typically containing Et_3N (see Table 3), to give substrate:complex molar ratios of 100:1. The resulting mixtures were aerated by stirring vigorously for 24h. At the conclusion of each reaction period, the mixture was concentrated to dryness *in vacuo* and the residue analysed by ^{1}H NMR spectroscopy to determine

the substrate:product ratio. After analysis of the residue, diethyl ether was added to dissolve and remove 3,5-DTBC and 3,5-DTBQ from the complex. Recyclability was established by adding fresh substrate, DMF and Et_3N to the complex from the initial reaction, and stirring for 24 h. The solvent was evaporated *in vacuo* and the residual material analyzed as before.

Acknowledgements

We are grateful to NRF, MINTEK and Rhodes University for generous financial support and Ms Leanne Cook (University of the Witwatersrand) for X-ray structure analysis.

References

1. Magnus, K. A.; Ton-That, H; Carpenter, J. E. *Chem. Rev*. **1994**, *94*, 727.
2. Karlin, K. D.; Gultneh,Y. *J. Chem. Ed*. **1985**, *62*, 983.
3. Solomon,E. I.; Sundaram, U. M.; Machonkin, T. E. *Chem. Rev*. **1996**, *96*, 2563.
4. Wellington, K. W. PhD Thesis, Rhodes University, 1999.
5. Kaye, P. T.; Nyokong, T.; Watkins, G. M.; Wellington, K. W. *ARKIVOC* **2002,** *(ix)*, 9.
6. Dismukes, G. C. *Chem. Rev.* **1996**, *96*, 2909.
7. Kim, E. E.; Wyckoff, H. W. *J. Mol. Bio.* **1991**, *218*, 449.
8. Christianson, O. W.; Lipscomb, W. N. *Acc. Chem. Res*. **1989**, *22*, 62.
9. Lipscomb, W. N.; Strater, N. *Chem. Rev.* **1996**, *96*, 2375.
10. Wilcox, D. E. *Chem. Rev*. **1996**, *96*, 2435.
11. (a) Sumner, J. B. *J. Biol. Chem.* **1926**, *69*, 435. (b) Volkmer, D.; Hörstman, A.; Griesar, K.; Haase, B.; Krebbs, B. *Inorg. Chem*. **1996**, *35*, 1132.
12. Fenton, D. E. In *Biocoordination Chemistry*, Oxford University Press: New York, 1995, p 29.
13. Burton, S. G.; Kaye, P. T.; Wellington, K. W. *Synth. Commun.* **2000**, *30*, 511.
14. Kaye, P. T.; Wellington, K. W. *Synth. Commun.* **2001**, *31*, 1.
15. Kaye, P. T.; Wellington, K. W. *Synth. Commun.* **2001**, *31*, 2405.
16. Burton, S. G. Ph.D Thesis, Rhodes University, 1993.
17. Thornton, D. A. *J. Coord. Chem.* **1991**, *24*, 142.
18. See, for example, Herr, H.; Spahl, W.; Trojandt, G.; Steglich, W.; Thaler, F.; van Eldik, R. *Bioorganic & Medicinal Chemistry* **1999**, *7*, 699. Pesavento, R. P.; Pratt, D. A..; Jeffers, J.; van der Donk, W. A. *J. Chem. Soc*., *Dalton Trans.* **2006**, 3326.
19. Vigato, P. A.; Tamburini, S.; Fenton, D. E. *Coord. Chem. Rev.* **1990**, *106*, 25.
20. Chyn, J. P.; Urbach, F. L. *Inorg. Chim. Acta* **1991**, *189*, 157.
21. Oishi, N.; Nishida,Y.; Ida, K.; Kida, S. *Bull. Chem. Soc. Japan* **1980**, *53*, 2847.
22. Kaye, P. T.; Watkins, G. M.; Wellington, K. W. *S. Afr. J. Chem*. **2005**, *58*, 1.

23. Triller, M. U.; Pursche, D.; Hsieh, W. Y.; Pecoraro, V. L.; Rompel, A.; Krebs, B. *Inorg. Chem.* **2003**, *42*(20), 6274.
24. Kovala-Demertzi, D.; Hadjikakou, S. K.; Demertzis, M. A.; Deligiannakis, Y. *J. Inorg. Biochem.* **1998**, *69*, 223.
25. Reported as the hydrochloride salt by Nandi, M. M.; Ray, R. *Indian Journal of Chemistry, Section B: Organic Chemistry Including Medicinal Chemistry* **1986**, *25B*(2), 222; *Chem. Abstr*. **1987**, *106*, 138323.
26. Kaptein, B.; Barf, G.; Kellogg, R. M.; Van Bolhuis, F. *J. Org. Chem*. **1990** *55*, 1890.
27. Hankovszky, H. O.; Hideg, K. *J. Med. Chem*., **1966**, *9*, 151; *Chem. Abstr*. **1966**, *64*, 35747.
28. Burton, S. G.; Kaye, P. T.; Wellington, K. W. *Synth. Commun*. **2000**, *30*, 511.
29. Sheldrick, G. M. *SHELX97, Program for the Refinement of Crystal Structures,* University of Gottingen, Germany.